Received: 14 November 2023 | Revised: 13 January 2024 | Accepted: 15 January 2024

DOI: 10.1111/adb.13375

ORIGINAL ARTICLE

Addiction Biology SSA WILEY

Roles of lncLingo2 and its derived miR-876-5p in the acquisition of opioid reinforcement

Hongyu Yang[1] | Xiuning Zhang[1] | Minglong Zhang[1,2] | Yun Lu[1] | Bing Xie[1] | Shaoguang Sun[3,4] | Hailei Yu[1] | Bin Cong[1] | Yixiao Luo[5] | Chunling Ma[1,4] | Di Wen[1,4]

[1]College of Forensic Medicine, Hebei Medical University, Hebei Key Laboratory of Forensic Medicine, Collaborative Innovation Center of Forensic Medical Molecular Identification, Research Unit of Digestive Tract Microecosystem Pharmacology and Toxicology, Chinese Academy of Medical Sciences, Shijiazhuang, Hebei Province, China

[2]Department of Genetics, Qiqihar Medical University, Qiqihar, Heilongjiang Province, China

[3]Department of Biochemistry and Molecular Biology, Key Laboratory of Medical Biotechnology of Hebei Province, Hebei Medical University, Shijiazhuang, China

[4]Key Laboratory of Neural and Vascular Biology, Ministry of Education, Shijiazhuang, Hebei Province, China

[5]Hunan Province People's Hospital, The First-Affiliated Hospital of Hunan Normal University, Changsha, China

Correspondence
Di Wen and Chunling Ma, Key Laboratory of Neural and Vascular Biology, Ministry of Education, Hebei Province, Shijiazhuang 050017, China.
Email: wendi01125@hebmu.edu.cn and chunlingma@hebmu.edu.cn

Yixiao Luo, Hunan Province People's Hospital, The First-Affiliated Hospital of Hunan Normal University, Changsha 410081, China.
Email: luoyx@hunnu.edu.cn

Funding information
National Natural Science Foundation of China, Grant/Award Number: 81971785; Natural Science Foundation of Hebei Province, Grant/Award Number: H2022206026

Abstract

Recent studies found that non-coding RNAs (ncRNAs) played crucial roles in drug addiction through epigenetic regulation of gene expression and underlying drug-induced neuroadaptations. In this study, we characterized lncRNA transcriptome profiles in the nucleus accumbens (NAc) of mice exhibiting morphine-conditioned place preference (CPP) and explored the prospective roles of novel differentially expressed lncRNA, lncLingo2 and its derived miR-876-5p in the acquisition of opioids-associated behaviours. We found that the lncLingo2 was downregulated within the NAc core (NAcC) but not in the NAc shell (NAcS). This downregulation was found to be associated with the development of morphine CPP and heroin intravenous self-administration (IVSA). As Mfold software revealed that the secondary structures of lncLingo2 contained the sequence of pre-miR-876, transfection of LV-lncLingo2 into HEK293 cells significantly upregulated miR-876 expression and the changes of mature miR-876 are positively correlated with lncLingo2 expression in NAcC of morphine CPP trained mice. Delivering miR-876-5p mimics into NAcC also inhibited the acquisition of morphine CPP. Furthermore, bioinformatics analysis and dual-luciferase assay confirmed that miR-876-5p binds to its target gene, *Kcnn3*, selectively and regulates morphine CPP training-induced alteration of *Kcnn3* expression. Lastly, the electrophysiological analysis indicated that the currents of small conductance calcium-activated potassium (SK) channel was increased, which led to low neuronal excitability in NAcC after CPP training, and these changes were reversed by lncLingo2 overexpression. Collectively, lncLingo2 may function as a precursor of miR-876-5p in NAcC, hence modulating the development of opioid-associated behaviours in mice, which may serve as an underlying biomarker and therapeutic target of opioid addiction.

Hongyu Yang, Xiuning Zhang and Minglong Zhang made equal contributions to this study.

KEYWORDS
addiction, *Kcnn3*, lncLingo2, miR-876-5p, nucleus accumbens, opioids

1 | INTRODUCTION

Opioids, which include morphine, are extensively utilized in therapeutic settings for the purpose of managing acute and chronic severe pain. Nevertheless, repeated opioid administrations will lead to addiction, which limits their clinical use. The term, drug addiction, is defined as a sort of maladaptive behaviours that are determined by the obsessive and uncontrolled use of drugs. Additionally, it has been observed that drug addiction can lead to the formation of powerful abnormal drug-related memories, which perform a specific function in the progression from initial drug exposure to the acquisition of drug reliance.[1,2]

Extensive studies using a variety of learning paradigms in animal models, including conditioned place preference (CPP) and intravenous self-administration (IVSA), have provided evidence suggesting that discrete neural systems are responsible for mediating different forms of learning and memory.[3,4] Furthermore, the processes involved in drug-associated memory are similar to those of non-drug-associated memories, including development, consolidation, retrieval, reconsolidation and extinction.[5–7] When individuals are subjected to addictive substances, the enduring emotional memory imprints that are established in the brain immersing the euphoric sensations generated by the drugs are involved in the pathological process of learning that underlies drug addiction.

Previous studies demonstrated that the formation of drug-associated memory is promoted by various distinct neural systems, including the amygdala, nucleus accumbens (NAc) and hippocampus.[8–10] The NAc lies in the ventral striatum particularly and is the key area in transforming intricate reward-related information into motivated behaviours. Furthermore, the NAc exhibits heterogeneity in its organization, with distinct core and shell subregions, and guides distinct behaviours due to their different cellular compositions and connection frameworks. Due to the distinct dopamine receptor 1- and receptor 2-expression, the NAc subregions have dissociative roles in the process of acquiring, reconsolidating and extinguishing drug-conditioned responses. For example, the NAc core (NAcC) is involved in the acquisition of morphine CPP, but the NAc shell (NAcS) is necessary for the reconsolidation of morphine CPP in mice.[11,12] These suggest that the NAc performs a crucial function in the manifestation of drug-related behaviours.[13–15] However, the detailed molecular mechanism underlying the learning and memory of drug-related scenarios in different NAc subregions remains largely unknown.

It is known that the persistent neuroadaptations induced by drugs in the NAc indicate that malfunctions in gene regulatory networks may be responsible for the development of drug memory and the acquisition of drug-related behaviours.[10,16] Recent studies have found that non-coding RNAs (ncRNAs), involving microRNAs (miRNAs), circular RNAs (circRNAs) and long non-coding RNAs (lncRNAs), play crucial roles in drug addiction by epigenetic regulation of gene expression.[17–19] lncRNAs, which are a class of non-coding transcripts with a length exceeding 200 nucleotides, manifest their biological activities through interactions with mRNAs, coupling with transcription factors and serving as competitive endogenous RNAs (ceRNAs). In addition, a complex interplay between these modulatory ncRNAs has been explored, wherein certain lncRNAs undergo processing to generate miRNAs that subsequently inhibit the expression of target mRNAs and play critical roles in the regulation of neural development and disease.[20] It has been observed that the abnormal expression of lncRNAs in the NAc performs an essential function in the mechanism of action of methamphetamine or cocaine-induced neural plasticity alteration and addiction.[21,22] Li et al found lncRNA–miRNA–mRNA interactions in the NAc were related to morphine addiction in mice by using transcriptomic analysis.[23] The overexpression of lncRNA MEG3 in response to morphine-induced autophagy in HT22 cells may occur through increasing c-fos expression and mediating the activation of ERK pathway.[24] Furthermore, some studies have identified expression changes miRNAs after chronic opioid exposure.[25] Therefore, we characterized miRNA, lncRNA and mRNA transcriptome profiles in NAc of morphine CPP-trained mice by RNA sequencing (RNA-Seq) in a preliminary study and found a novel lncRNA, lncLingo2, was highly expressed in NAc and significantly downregulated after morphine CPP training. Furthermore, bioinformatic analysis revealed that lncLingo2 could derive miR-876-5p generation. Further clarification is required on the involvement of lncLingo2 and its derived miR-876-5p in drug memory formation and the acquisition of drug-associated behaviours.

Throughout the current investigation, we first proved the correlation between lncLingo2 and miR-876-5p, then trained mice with morphine CPP and paradigms of the heroin IVSA for examining the function and the fundamental mechanisms of lncLingo2, and it derived miR-876-5p in the NAc during the development of drug memory and acquisition of drug-related behaviours.

2 | MATERIALS AND METHODS

2.1 | Animals

Specific pathogen-free (SPF) wild-type C57BL6/N male mice weighing between 22 and 25 g and aged 10 weeks old have been procured from Liaoning Changsheng Co. Ltd (Liaoning, China). The animals underwent a 12-h light and dark cycle, with the lights being turned off at 7:00 AM. During this time frame, the animals were provided with unhindered availability of food and drink. The normal temperature of

room was consistently regulated at 22 ± 1°C, while the relative humidity was maintained at around 60%. The mice underwent a period of acclimation to the laboratory environment for 1 week prior to experimental procedures. The behavioural trials were performed throughout the dark cycle. The study was granted approval from the Institution Animal Care and Use Committee of Hebei Medical University (agreement number: 2018010), and all procedures were conducted in accordance with the guidelines of National Research Council Guide for the Care and Use of Laboratory Animals.

2.2 | Drugs

Morphine sulphate was purchased from Qinghai Pharmaceutical Factory (Qinghai, China), and heroin was supplied by the Beijing Municipal Public Security Bureau in China. The drug concentrations were modified to provide a suitable injection volume of 10 mg/kg body weight using saline solution. The preparation of fresh drug solutions was on the day of administration.

2.3 | Behavioural tests

2.3.1 | CPP test

The CPP test was performed using an experimental setup consisting of two compartments that were capable of being separated by guillotine doors. The two chambers exhibited clear visual and tactile differences. One chamber (15 × 15 × 30 cm) had vertical black and white stripes using 3 cm wide stripes and a floor exhibiting rough polyvinyl chloride mesh (0.8 × 0.8 cm), whereas the remaining chamber (15 × 15 × 30 cm) exhibited horizontal black and white stripes walls with 3 cm wide stripes and a floor with smooth polyvinyl chloride mesh (0.8 × 0.8 cm). A guillotine door was utilized to connect two identically sized compartments. During the CPP test, the SMART video tracking system (Panlab Technology for Bioresearch, Spain) was used to automatically record animal behaviour. The CPP scores represent the difference between the duration spent in the morphine-paired compartment and the duration spent in the saline-paired compartment on the designated test day. Adaptive capture was taken for 3 days before starting the CPP training. The experimental procedure encompassed three different stages: pre-conditioning, conditioning and testing. Pre-conditioning: On day 1, all animals were situated in the middle of whole equipment and permitted unrestricted access to the whole equipment for a duration of 15 min. The CPP scores were computed at the baseline (T0). Animals with initial side bias (i.e., CPP scores more than 150 s) were not included in the investigation. Conditioning: This phase spanned a period of 6 days (from days 1–6). Intraperitoneal injection of morphine (10 mg/kg) or saline (10 ml/kg) has been administrated throughout the morning (09:00) and afternoon (15:00) (6-h apart). Following every application of the injection, the participants were promptly restricted to the respective drug-associated or saline-associated section of the CPP chamber for a duration of 45 min. Testing: The post-conditioning test was conducted on day 7 while the subjects were in a state free from the influence of morphine. The mice were introduced into the chambers, wherein the guillotine doors had been eliminated, so granting unrestricted access to the entire apparatus for a duration of 15 min.

2.3.2 | IVSA test

Operant chambers (22 × 22 × 25 cm, Shanghai Vanbi Intelligent Technology Co., Ltd.) were positioned within sound attenuation cubicles. Every operant chamber included two levers on one side of the chamber and a food receptacle on the chamber's opposite side. The experimental subjects were consisted of animals that underwent testing under a fixed-ratio 1 (FR1) schedule, with every testing round having a duration of 60 min. The lever on the right was labelled as the 'active' lever, and it resulted in the administration of a heroin injection (25 μg/kg) at a constant rate of 0.005 ml/s for a period of 4 s when pressed. On the other hand, the lever on the left was labelled as the 'inactive' lever, and it was ineffective but still documented. The cue light was positioned above the right lever, and the initiation of cue light signified the delivery of heroin. Following the administration of heroin, the cue light was deactivated, initiating a 5 s interval with no drug was accessible. The experimental variables of IVSA were coded utilizing Trigger Master V3.0 (Shanghai Vanbi Intelligent Technology Co., Ltd.).

Before IVSA training, the mice were subjected to the placement of indwelling catheters in the right jugular vein, following the previously established protocol.[26] Subsequently, a recovery period of 3 days was provided. Following the surgical procedure and subsequent recuperation duration, mice were subjected to an IVSA using heroin for a duration of 7 days. The patency of catheter was assessed by administering 4 mg/kg propofol injectable emulsion every 3 days throughout the training period, as well as at its conclusion. Catheters were considered patent just when mice exhibited the loss of righting reflex within a time frame of 3 s subsequent to the injection. Mice that did not pass the patency test at any given time points were rejected from the investigation.

2.3.3 | Glucose pellets self-administration

Operant chambers were the same as those used in the heroin IVSA test. Mice were firstly weighed (free feeding weight) and then were food restricted (2 mg per day; 3–4 days). Glucose pellets SA experiments followed the same protocol designed as heroin IVSA experiments with the exception that mice were received a glucose pellet instead of heroin delivery. Mice were first trained for glucose pellets reinforced lever responding until responding met baseline criteria adopted from previous study.[26] After restricting diet phase, mice were trained for glucose pellets SA for a period of 7 days. Behavioural variables consisting of the number of active and inactive lever presses

and number of glucose pellets delivered were assessed. Glucose pellet SA experimental variables were programmed using Trigger Master V3.0 (Shanghai Vanbi Intelligent Technology Co., Ltd.).

2.3.4 | Locomotion test

Mice were placed in the center of the open field chamber (25 × 25 × 30 cm), and the travelled distance was analysed by SMART video tracking system (Panlab Technology for Bioresearch, Spain) for 15 min. The chambers were cleaned with 70% ethanol solution to remove odour cues after each test.

2.4 | Quantitative reverse transcription PCR (qRT-PCR)

The NAcC tissue has been obtained from brain sections of approximately 600 μm using a micro punch instrument (BT1.0, Harris, USA). The NAcS underwent dissection using a needle, following the guidance provided by the mouse brain atlas. The total RNAs were extracted using RNAiso plus agent (Takara, Japan) and reversely transcribed with the Primescript RT reagent kit (Takara, Japan) or miScript II RT Kit (Qiagen, USA). Primer sets utilized within qRT-PCR assays are manufactured by Sangon Biotech (Shanghai, China), and Table 1 presents the primer's sequences. The other primers specific for U6 and the miRNAs were purchased from RiboBio (Guangzhou, China).

TABLE 1 Information of primers for qRT-PCR.

Name	Primers
LncLingo2	F: AGCTGTGTGGAAAGGCCCTA R: TCCACTCAACGTGAAGCTCAA
LncRNA4	F: TCAGCACGTTTGGTGGAGAG R: GATGTCAACTTGCCCAAGGC
LncRNA8	F: TGGCCACTGTCGTGTAGATG R: AACTCCAGAAGTCGGTCTGC
LncRNA11	F: CATCAGACTCCAGGGCCAAT R: CAGGATTCCCAGGCAAAGGA
LncRNA14	F: GTTTGGCATGTCTCAGCAGTC R: TGAAGAGCATCCCGAGTTCA
GAPDH	F: GGTGAAGGTCGGTGTGAACG R: CTCGCTCCTGGAAGATGGTG
U6	F:GGAACGATACAGAGAAGATTAGC R:TGGAACGCTTCACGAATTTGCG
UNC5C	F: GTGCGGCAGGTTGAAGGAGAAG R: GCAGGGTCCAGGAGAGGTAAGTC
ALX1	F: CTAGCGGTGGTTCTGTGGTTACG R: TGTCCGAGGCGAGTGAGAGTAAG
SEMA6A	F: AGATGCAACACTCCTCCTCCTATGG R: GTGGTCTGGTGGCTTCTTGTGAG
KCNN3	F: GGCAACTGTGGCACGGAAGAC R: AAGACACGAGACAGCAGCATCAAG

A Q7 Real-Time PCR machine (Applied Biosystems, USA) was utilized for amplification and detection. Two different methods were employed: the TB Green Premix Ex Taq II method (Takara, Japan) and the miScript SYBR Green PCR Kit method (Qiagen, USA). The relative expression levels of lncRNA, mRNA and miRNA were determined by employing the $2^{-\Delta\Delta Ct}$approach. The expression values were normalized by employing GAPDH or U6 as the internal control.

2.5 | 3′- and 5′-Rapid amplification of cDNA ends (RACE)

3′- and 5′-RACE has been utilized to identify transcriptional initiation sites of lncLingo2 employing M-MuLV First Strand cDNA Synthesis Kit M-MuLV (B532435), LA Taq (TaKaRa, DRR02AG) and Marker (BBI, B600032), 6 × DNA Loading Dye (Sangon Biotech), and Sanprep Column DNA Gel Extraction Kit (B518131, Sangon Biotech, China) has been employed for sequencing based on the manufacturer's guidelines. Two reverse primers for the TSS of lncLingo2 have been utilized in a nested PCR with the two 5′ primers (5′ outer GCTGTCAACGATACGCTACGTAAC, 3′ inner GCTACGTAACGGCATGACA GTG) from the kit.

2.6 | Subcellular fractionation

The process of subcellular fractionation has been conducted following the instructions provided by the cytoplasmic and nuclear RNA purification kit (Norgen Biotek, Ontario). The cytoplasmic reference GAPDH and the nucleus reference U6 were utilized in the study. The quantification of lncLingo2 expression levels in the specified fractions was performed using qRT-PCR. The experiment was replicated three times in duplicate.

2.7 | RNA fluorescence in situ hybridization (FISH)

The expression of LncLingo2 in the NAc area has been conducted using the lncRNA FISH Kit (Norgen Biotek, Canada) based on the manufacturer's guidelines. We followed the detailed protocol provided in the kit. Briefly, the brain tissues of mice underwent fixation in 4% paraformaldehyde (Sigma, USA) for a duration of 48 h and underwent dehydration, paraffin-embedded and sectioned. After incubating the tissue with the probes for lncLingo2 (Servicebio, China) for 4 h at 37°C, and conducted various hydrating steps. Tissue was counterstained via DAPI, and findings underwent visualization utilizing the Leica confocal microscope system (Leica SP8, German).

2.8 | Bioinformatics analysis

The secondary structure of lncLingo2 has been anticipated by Mfold (http://www.bioinfo.rpi.edu/applications/mfold). The identification of

target genes was accomplished by the utilization of bioinformatics software tools, such as miRDB, TargetScan (http://www.targetscan.org/mmu_72/) and microT-CDS (http://diana.imis.athena-innovation.gr/DianaTools).

2.9 | Dual-luciferase reporter assays

The HEK293 cell line was employed to perform the dual-luciferase reporter vector tests. A fragment of the 3′ untranslated region (3′ UTR) of *Kcnn3* gene, which includes the anticipated binding site for miR-876-5p, was subcloned into the luciferase reporter vector. The miR-876-5p mimic or a mimic negative control was co-transfected with the vector into HEK293 cells utilizing Lipofectamine 2000 (Invitrogen, USA). After 48 h of transfection, cells were lysed using 0.5% trypsin, and luciferase activity underwent assessment utilizing a dual-luciferase reporter assay kit (Transgen, China). The data were subjected to normalization using control groups that underwent treatment with *Kcnn3* wild-type and miR-876-5p scramble vectors.

2.10 | Western-blot assay

The researchers performed animal sacrifices through decapitation and afterwards collected NAc core tissues. The denatured total protein from all samples was subjected to separation employing a specific SDS–PAGE technique, with equal quantities being employed for each sample. The proteins that had been isolated were subsequently deposited onto a nitrocellulose membrane with a pore size of 0.2 μm. The membranes underwent inhibition via 5% skim milk in TBS solution and incubated via specific primary antibodies against anti-KCNN3 (N-term) (1:800, Alomone Labs, Israel). GAPDH (1:1000, Proteintech, China) has been employed as an internal control to normalize the data. Then, the membranes underwent a washing step using TTBS and were subsequently subjected to incubation with a secondary antibody, specifically a fluorophore-conjugated goat anti-rabbit secondary antibody (1:10000, Rockland, USA). The fluorescence underwent evaluation employing the Odyssey LICOR gel system (LI-COR, USA). The determination of individual intensity bands was conducted utilizing the Image J Program Analyser (Media Cybernetics, USA).

2.11 | Lentiviral (LV) construction

Lentiviruses expressing lncLingo2 and control scramble vector have been designed and developed with standard techniques using Genechem (Shanghai, China). Lentiviral vector construction and viral particle packaging were performed by Genechem Technology (China). The lentiviral expressing lncLingo2 was LV- lncLingo2 and the control scramble was the empty lentiviral system with no sequence insertion.

2.12 | Stereotaxic surgery and microinjection

The mice were placed within a stereotactic frame (NeuroStar, German) and subjected to anaesthesia by isoflurane inhalation. A hole with a diameter of 0.5 mm was then drilled (AP: 1.42 mm; ML: ±1.00 mm; DV: 4.00 mm). The virus (0.2 μl) was injected using a 28-gauge needle attached to a micro-syringe pump controller at a constant rate of 0.02 μl/min. The co-injection of specific LVs (Genechem, China) together with a helper virus (Genechem, China) was performed in the NAcC. The injection sites were verified by fluorescence stereomicroscope, and animals with incorrect injection placement were excluded from analyses (fewer than 5% of animals). A behavioural test was performed 14 days after the LV injection when they were stably expressed. The LV-mediated overexpression of LncLingo2 in the NAcC was detected by qRT-PCR.

2.13 | Cannula attachment and microinjections

To facilitate drugs' direct injection into the NAcC, a guide cannula with certain dimensions (inner diameter: 0.34 mm, outer diameter: 0.48 mm) was surgically attached into the NAcC region of mice that were anaesthetised with isoflurane with (AP: 1.42 mm; ML: ± 1.00 mm; DV: 3.80 mm). Subsequently, the guiding cannula was affixed to the skull using dental cement. To prevent blockage, a dummy cannula was put into the guiding cannula. The microinjections were performed using a 10 μl syringe (Hamilton, USA), which was connected to a polyethylene (PE) tube. The PE tube was then connected to the injection cannula (inner diameter: 0.14 mm, outer diameter: 0.30 mm). The microinjections have been conducted at a rate of 0.02 μl/min, utilizing a syringe pump (KD Scientific, USA), with a total volume of 0.2 μl.

2.14 | Electrophysiology

The brain slice preparation procedure was conducted in accordance with the methods previously outlined.[27] The brains were sectioned into coronal slices with a thickness of 250 μm utilizing a Leica VT1200S vibratome (Leica, Germany) and cutting artificial cerebrospinal fluid (aCSF). The slicing of aCSF consisted of 93mM N-methyl-d-glutamine diatrizoate, 20 mM HEPES, 25 mM glucose, 2.5 mM KCl, 10 mM $MgSO_4$, 0.5 mM $CaCl_2$, 1.2 mM NaH_2PO_4, 30 mM $NaHCO_3$, 3 mM pyruvate, 2 mM thiourea and 5 mM ascorbate. The brain sections underwent incubation within holding aCSF containing 20 mM HEPES, 92 mM NaCl, 2.5 mM KCl, 2 mM $CaCl_2$, 1 mM $MgCl_2$, 30 mM $NaHCO_3$, 1.2 mM NaH_2PO_4, 3 mM pyruvate, 2 mM thiourea, 25 mM glucose and 5 mM ascorbate. During the recording, the slices containing NAc were incubated in recording aCSF comprising 126 mM NaCl, 3 mM KCl, 1.5 mM $MgCl_2$, 2.4 mM $CaCl_2$, 11 mM glucose, 1.2 mM NaH_2PO_4 and 26 mM $NaHCO_3$. The neurons of NAcC were observed utilizing differential interference contrast/infrared illumination using a fixed-stage upright microscope. Electrophysiological signals have been

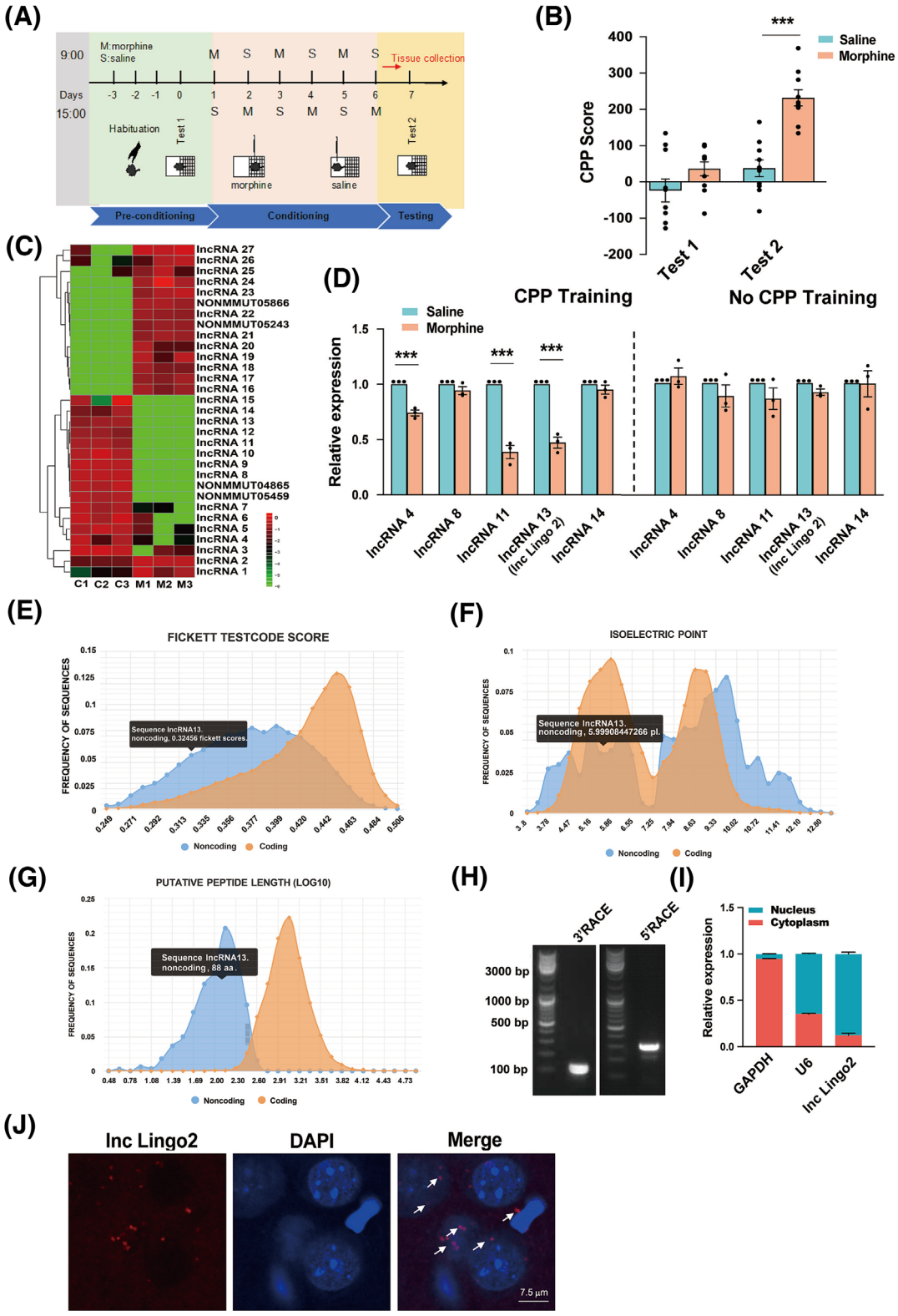

FIGURE 1 Legend on next page.

documented on Clampex 10.1 and an Axon 700B patch amplifier (Axon Instruments, USA). Throughout the slice preparation and recording, the slices were continuously maintained with a constant flow of 95% O_2 and 5% CO_2 at 34 °C.

To measure the tail current mediated by the SK channel, neurons were maintained at a membrane potential of −70 mV and thereafter subjected to a depolarization period of 300 ms. The depolarization voltages varied from −50 to 0 mV in decrements of 10 mV. The tail current manifests at the restoration of action potential to a membrane potential of −70 mV. The action potential (AP) firing was measured using a current clamp protocol. The neurons were maintained at −60 mV and evoked by sequential current injections ranging from 0 to 400 pA with 20 pA increasing increments for 400 ms per sweep. In order to quantify the AHP, the minimum amplitude of current was modified for every individual cell to confirm that the first pulse occurred before reaching the threshold for spike firing. The intracellular solution described above was composed of a concentration of 2 mM KCl, 3 mM $MgCl_2$, 140 mM K-gluconate, 10 mM HEPES, 5 mM tris-phosphocreatine, 2 mM K-ATP and 0.2 mM Na-GTP.

2.15 | Statistical analysis

All data were tested using Kolmogorov–Smirnov and Shapiro–Wilk tests, to verify that the data conformed normal distribution. The behavioural data were subjected to independent one- or two-way ANOVA, deemed suitable, and analysed with Bonferroni's post hoc tests afterwards. Gene (lncRNA, miRNA and mRNA) and the expression levels of protein have been investigated using *t*-tests in order to conduct two-group comparisons and one-way ANOVAs for performing multiple groups comparisons. Meanwhile, the abnormal distributed data were analysed using non-parametric tests. All outcomes have been presented as the mean ± SEM after analyses via Prism 8 software.

3 | RESULTS

3.1 | LncLingo2 expression in NAc decreases after morphine CPP training

In order to examine the alteration within lncRNAs expression correlated with drug-associated behaviour in morphine CPP, 26 mice divided into two distinct groups underwent conditioning using saline (2 ml/kg) or morphine (10 mg/kg) treatments (Figure 1A). In consideration of the effects of drug memory consolidation on lncRNAs expression during CPP post-test, 10 mice were tested for morphine CPP and three mice had their heads cut off for the collection of NAc tissues 1 h after the last CPP training. Analysis of two-way ANOVAs demonstrated the significant impact of morphine treatments ($F_{1,\ 18} = 42.01$, $p < 0.001$), test phase ($F_{1,\ 18} = 29.24$, $p < 0.001$) and integration among two factors ($F_{1,\ 18} = 8.902$, $p = 0.008$). The outcomes obtained from post hoc tests revealed that the CPP scores in test 2 of morphine-paired mice were much higher than saline-paired mice in the present morphine CPP paradigm ($p < 0.001$) (Figure 1B). Subsequently, lncRNA sequencing was performed on three samples of the NAc tissue within each experimental group. The results showed that 14 lncRNAs have been overexpressed and 17 have been underexpressed, as shown in the heatmap (Figure 1C). Validation of five downregulated lncRNAs expression has been conducted via qRT-PCR analysis which validated three (lncRNA4/lncRNA11/lncRNA13, $p < 0.001$) out of five lncRNAs were downregulated (Figure 1D) after CPP training, and no significant variation has been demonstrated among saline and morphine treated mice without CPP training.

Herein, lncRNA13 was selected for the following study, and RACE analysis showed that lncRNA13 is 3,900 nucleotides in length (Figure 1H). Alignments using the UCSC genome browser showed that the lncRNA13 sequence is poorly conserved among species and is located on the chromosome 4 and located on a gene named Lingo2. Therefore, we name it lncLingo2. Then, the LncLingo2 coding potential was predicted utilizing the online tool Coding Potential Calculator 2.0. The Fickett score of the lncLingo2 sequence was 0.32456, the complete putative ORF was 88 AAs and the isoelectric point was 5.9990844, which indicated its non-coding potential (Figure 1E–G). For detecting the cellular localization of lncLingo2, subcellular fractionation was separated, and the results obtained from qRT-PCR demonstrated that lncLingo2 had been primarily distributed within the cell nucleus (Figure 1I). FISH analysis also indicated that lncLingo2 was primarily located in the cell nucleus (Figure 1J).

3.2 | LncLingo2 in NAcC, but not in NAcS, regulates the acquisition of morphine CPP

Due to the different functions of NAcC and NAcS (Figure 2A) across the attainment of addictive behaviours, the alterations in the expression of lncLingo2 within these subregions were detected on 1, 3 and

FIGURE 1 LncLingo2 expression decreases in the NAc after morphine CPP training. (A) Experimental timeline of morphine CPP training and tissue collection. (B) CPP degrees increased within analysis 2 following 6 days of morphine CPP training ($n = 10$ per group). ***$p < 0.001$ vs. saline group. (C) The heatmap exhibiting clusters of lncRNAs differentially expressed in NAc tissue samples between saline and morphine CPP-trained mice. Fourteen of the lncRNAs have been elevated, and 17 have been reduced (fold change ≥ 2 and $p < 0.05$). (D) The expression of five downregulated lncRNAs in NAc was detected after morphine CPP training and only morphine treatment without CPP training, respectively ($n = 3$ per group). ***$p < 0.001$ vs. saline group. (E) The Fickett testcode score of lncLingo2 in mice. (F) The isoelectric point of lncLingo2 in mice. (G) The putative peptide length (Log10) of lncLingo2 in mice. (H) The amplification production of 3′ RACE and 5′ RACE was identified by agarose gel electrophoresis. (I) The analysis of lncLingo2 expression in subcellular fractionation ($n = 3$). The cytoplasmic reference GAPDH and the nuclear reference U6 were utilized in the study. (J) RNA FISH result showed lncLingo2 predominant localization in the cell nucleus. Scale bar = 7.5 μm.

6 h after the last morphine CPP training session. According to Figure 2B, analysis of one-way ANOVAs exhibited significant difference among groups ($F_{3,\ 16} = 23.07$, $p < 0.001$), and post hoc tests exhibited lncLingo2 expression within NAcC decreased at 1 h ($p < 0.001$) and 3 h ($p < 0.05$) after the last CPP training, but not at 6 h ($p > 0.05$), while the expression of lncLingo2 in NAcS had no difference ($F_{3,16} = 0.2315$, $p = 0.8731$).

To understand the possible functional activity of NAc LncLingo2 expression changes within the acquisition of morphine CPP, we performed lentivirus-mediated overexpression of LncLingo2 in NAcC and NAcS, respectively, before morphine CPP training (Figure 2C). The location of LV injection in NAcC and NAcS was validated via mCherry fluorescent protein visualization after behavioural tests (Figure 2D). Moreover, there is no significant difference in the locomotor activity after overexpression of LncLingo2 in NAcC ($t = 0.5565$, $p = 0.5830$) (Figure 2E).

The results of two-way ANOVAs demonstrated a significant main effect on CPP scores for morphine treatments ($F_{1,27} = 17.38$, $p < 0.001$) and overexpression of LncLingo2 in NAcC ($F_{1,27} = 43.90$, $p < 0.001$). Furthermore, there were observed interactions between

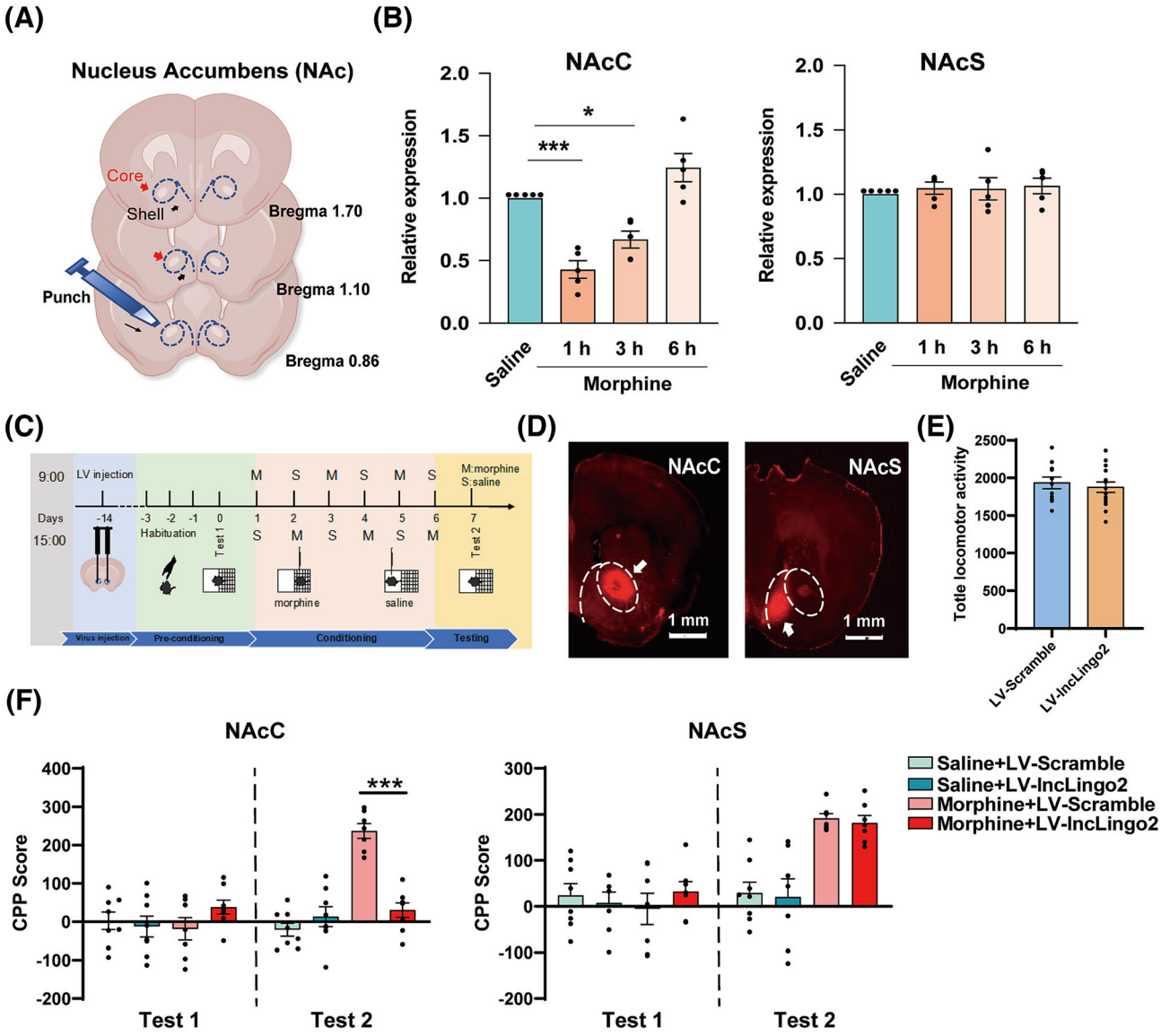

FIGURE 2 LncLingo2 in NAcC, but not in NAcS, regulates the acquisition of morphine CPP. (A) Reference images illustrating NAcC and NAcS subregions tissue collection. (B) The expression of lncLingo2 in NAcC, but not in NAcS, decreased in a time-dependent manner ($n = 5$ per group). ***$p < 0.05$; ***$p < 0.001$ vs. saline group. (C) Experimental timeline of LV microinjection and morphine CPP training. (D) The sketch map of lncLingo2 upregulating utilizing LV and GFP fluorescent protein exhibiting the location of LV microinjections within the NAcC and NAcS. Scale bar = 1 mm. (E) The effect of LV-lincgo2 overexpression on spontaneous activity in mice. The difference in the locomotor activity counts between the two groups was not significant ($n = 11$ and 15 for LV-scramble and LV-LncLingo2 groups, respectively). (F) Overexpression of lncLingo2 in the NAcC, but not NAcS, inhibited the attainment of morphine CPP ($n = 7$–8 per group). ***$p < 0.001$ vs. LV-scramble lncRNA group in morphine-trained mice.

morphine treatments × overexpression of LncLingo2 in NAcC ($F_{1,27} = 33.57$, $p < 0.001$). While in the experiment of overexpression LncLingo2 in NAcS, the result only indicated the main effect on CPP scores for morphine treatments ($F_{1,25} = 41.68$, $p < 0.001$), but not for overexpression of LncLingo2 in NAcS ($F_{1,25} = 0.1305$, $p = 0.7210$). According to Figure 2F, the resulting post hoc test revealed that viral promoted overexpression of LncLingo2 in the NAcC significantly inhibited the attainment of morphine CPP ($p < 0.001$), while LncLingo2 overexpression in the NAcS did not alter the CPP score ($p = 0.9932$) in test 2.

3.3 | LncLingo2 in NAcC is not involved in the acquisition of glucose pellets SA

To explore the role of lncLingo2 in natural rewarding behaviours, we developed the glucose pellets SA paradigm in mice (Figure 3A). Figure 3B showed the timeline of the glucose pellets SA paradigm, and then the NAcC tissue was collected after the seventh training day. According to Figure 3C and 3D, a repeated-measures two-way ANOVA exhibited significant main impact of glucose pellets ($F_{1,12} = 168.9$, $p < 0.001$) and training session ($F_{2.279,27.34} = 8.837$, $p = 0.0007$) on active lever presses (ALP) and glucose pellets (glucose: $F_{1,12} = 179.2$, $p < 0.001$; training session: $F_{2.607,31.28} = 4.200$, $p = 0.0165$), but not on inactive lever presses (ILP) (heroin: $F_{1,12} = 4.239$, $p = 0.0619$; training session: $F_{3.881,46.57} = 1.263$, $p = 0.2983$), suggesting that glucose intake increases as training progresses. Moreover, an unpaired t test analysis showed that there was no change of lncLingo2 expression in NAcC after glucose pellets SA training ($t = 0.6463$, $p = 0.5303$) (Figure 3E). The aforementioned findings indicated that lncLingo2 might not be related to the acquisition of glucose pellets SA.

3.4 | LncLingo2 in NAcC regulates the acquisition of heroin IVSA

We subsequently investigated the role of LncLingo2 in opioid-associated behaviours using the heroin IVSA paradigm. Figure 4A shows the schematic procedure of heroin IVSA. The mice underwent training to self-administer heroin at a dosage of 25 μg/kg/infusion using a fixed ratio 1 (FR-1) for 8 days. A repeated-measures two-way ANOVA exhibited significant main impact of heroin ($F_{1,10} = 31.71$, $p < 0.001$) and training session ($F_{2.008,20.08} = 5.464$, $p = 0.0127$) on

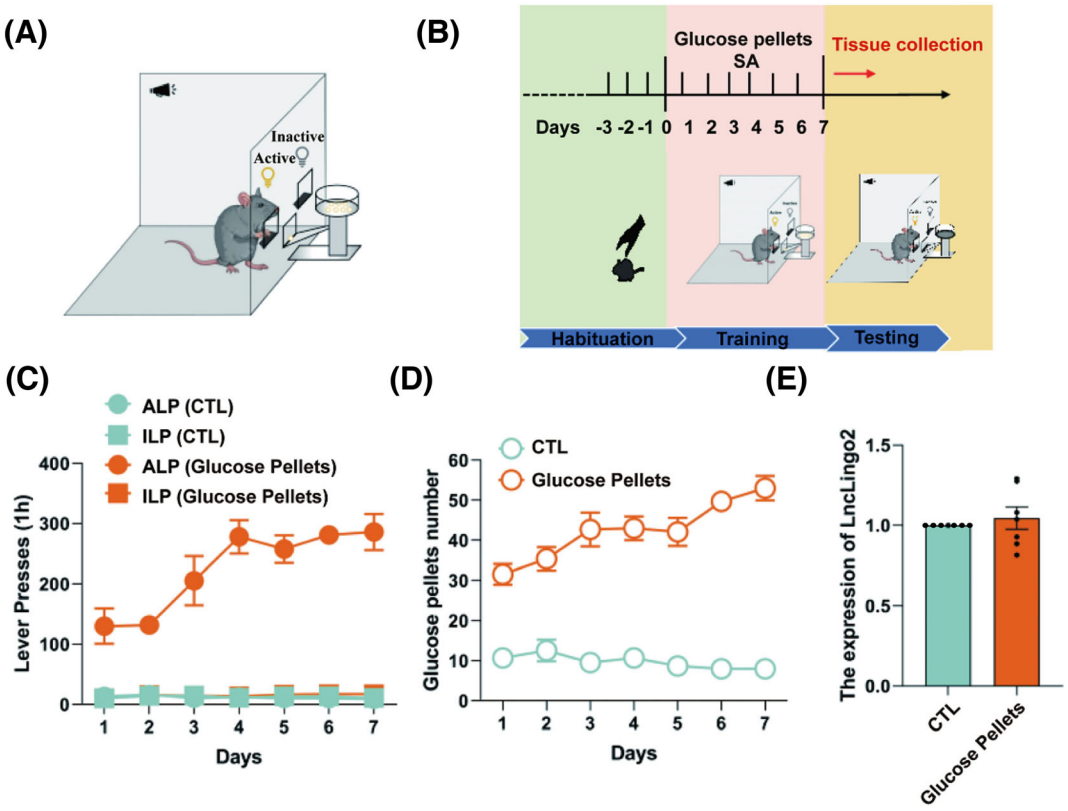

FIGURE 3 The expression levels of lncLingo2 in the NAcC after glucose pellets SA training. (A) Schematic illustration of glucose pellets self-administration. (B) Timeline of the glucose pellets SA paradigm. (C) The mean number of active and inactive lever-presses during the acquisition of glucose pellets SA training under 1 h FR1 schedules for 7 days ($n = 7$, per group). (D) The mean number of glucose pellets during acquisition of glucose pellets SA training under 1 h FR1 schedules for 7 days ($n = 7$, per group). (E) The expression levels of lncLingo2 in the NAcC after glucose pellets SA training ($n = 7$, per group).

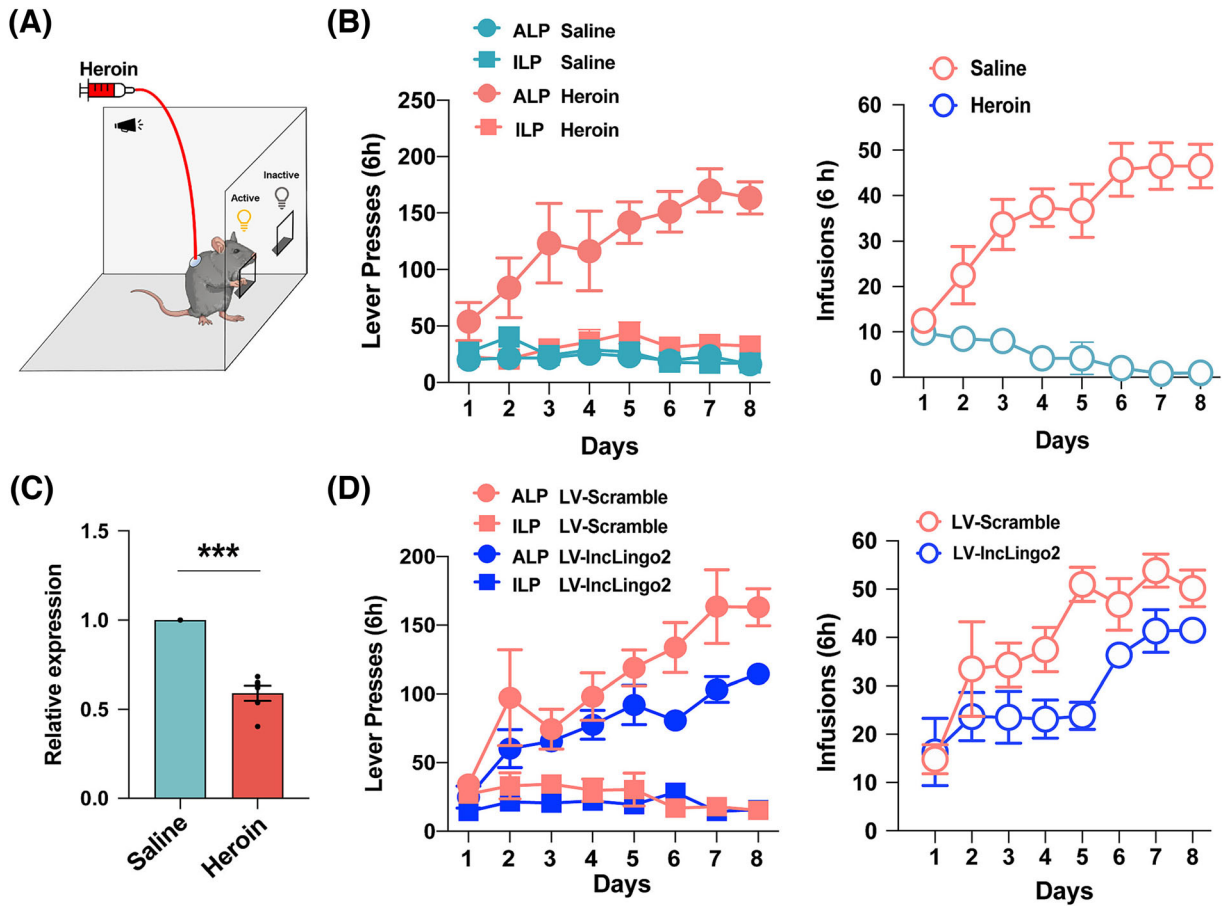

FIGURE 4 LncLingo2 in NAcC regulates the acquisition of heroin IVSA. (A) The schematic procedure of heroin IVSA. (B) The mean number of active and ILP (left) and infusions (right) during the acquisition of heroin IVSA training under 6-h FR1 schedules for 8 days ($n = 6$ per group). (C) LncLingo2 expression was significantly decreased in NAcC after heroin IVSA training ($n = 6$ per group). ***$p < 0.001$ vs. saline group. (D) Overexpression of lncLingo2 in the NAcC reduced ALP (left) and heroin infusions (right) during the acquisition of heroin IVSA ($n = 6$ per group).

active lever presses (ALP) and heroin infusions (heroin: $F_{1,10} = 65.54$, $p < 0.001$; training session: $F_{2.657,26.57} = 4.500$, $p = 0.0136$), but not on inactive lever presses (ILP) (heroin: $F_{1,10} = 1.435$, $p < 0.2585$; training session: $F_{3.093,30.93} = 0.9630$, $p = 0.4247$) (Figure 4B), indicating escalated heroin intake as the sessions progressed. In addition, there were interactions of heroin × training sessions on ALP ($F_{7,70} = 5.657$, $p < 0.001$) and heroin infusions ($F_{7,70} = 13.55$, $p < 0.001$). After heroin IVSA training, tissues of NAcC were immediately collected. Figure 4C shows that LncLingo2 expression in NAcC of heroin IVSA-trained mice was significantly decreased ($p < 0.001$).

Furthermore, LV-lncLingo2 was injected into NAcC for LncLingo2 overexpression and then performed heroin IVSA. Two-way ANOVA results (repeated measures) revealed a statistically significant main impact of training session ($F_{2.329,23.29} = 10.24$, $p < 0.001$) and lncLingo2 overexpression (F1,10 = 18.33, $p = 0.002$) on ALP and heroin infusions (training session: $F_{3.079,30.79} = 14.16$, $p < 0.001$; LncLingo2 overexpression: $F_{1,10} = 7.434$, $p = 0.021$) (Figure 4D). The aforementioned outcomes demonstrated that overexpression of lncLingo2 in NAcC also inhibited the acquisition of heroin IVSA, and lncLingo2 in NAcC played a role of opioid drug-associated behaviour.

3.5 | MiR-876-5p derived from lncLingo2 regulates the acquisition of morphine CPP

In view of the fact that the regulatory mechanism of lncRNA is closely related to its secondary structure, we predict the secondary structure of lncLingo2 by Mfold. According to the secondary structures diagram of lncLingo2, all seven categories of secondary structures contained the sequence of pre-miR-876, which was labelled by the red identifiers (Figure 5A). To verify whether lncLingo2 is the precursor of miR-876, we detect the precursor and mature miR-876 expression level after the HEK293 cell transfected with LV-lncLingo2 for 48 h. HEK293 cell line does not normally express lncLingo2. With the increased expression of lncLingo2 after LV-lncLingo2 transfection, the miR-876 precursor and mature miR-876 expression level also upregulated (Figure 5B). We hypothesized that lncLingo2 might be the miR-876 precursor. Then, we detected the expression of miR-876 in the NAcC and NAcS of mice after morphine CPP training. The aforementioned outcomes demonstrated that the pre-miR-876 ($F_{3,18} = 22.49$, $p < 0.001$), miR-876-3p ($F_{3,18} = 7.778$, $p = 0.002$), miR-876-5p ($F_{3,18} = 28.00$, $p < 0.001$) expression level within NAcC

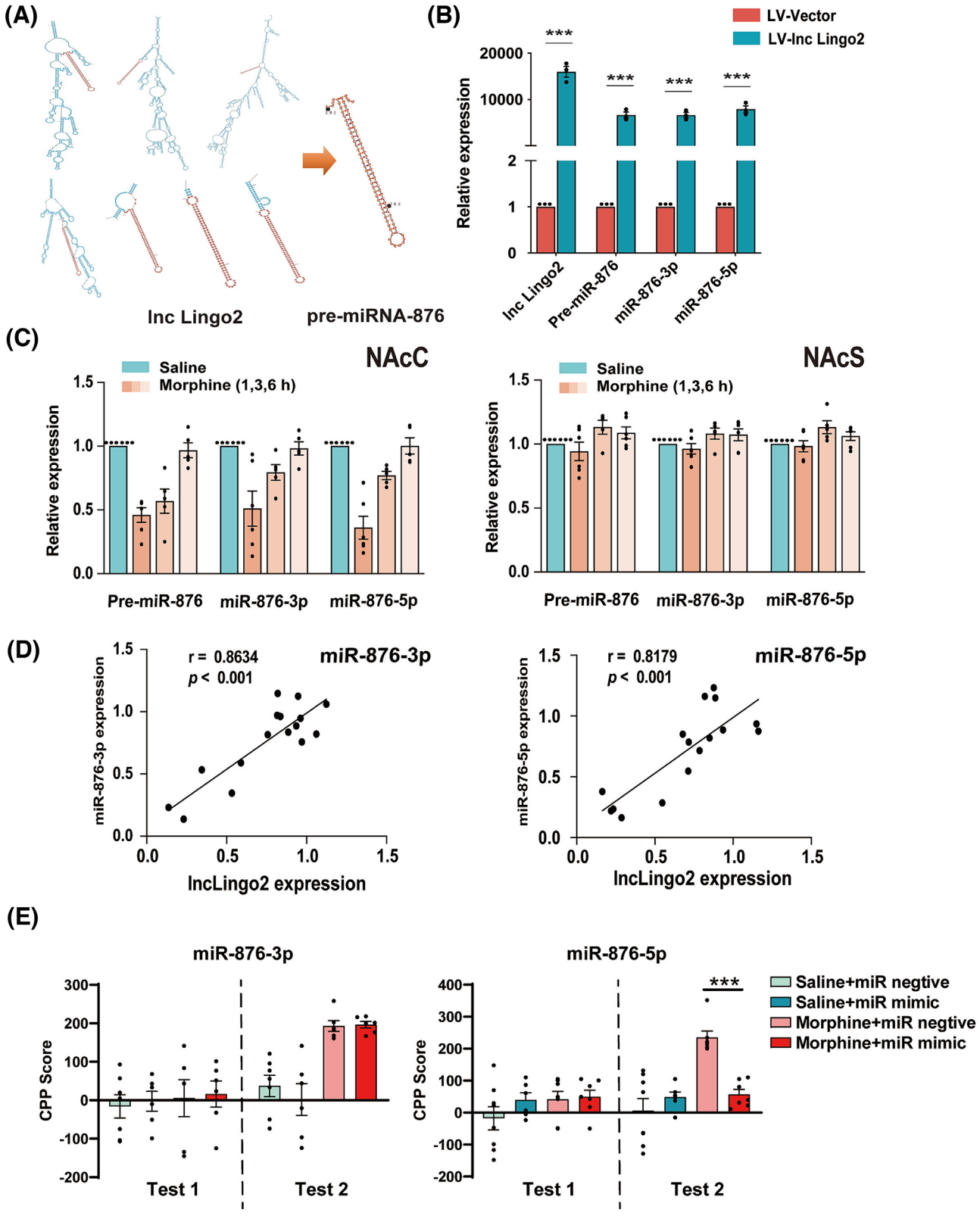

FIGURE 5 Legend on next page.

decreased in a time-dependent manner after CPP training but had no change in NAcS (pre-miR-876: $F_{3,18} = 2.547$, $p = 0.088$; miR-876-3p: $F_{3,18} = 1.871$, $p = 0.171$; miR-876-5p: $F_{3,18} = 2.128$, $p = 0.132$) (Figure 5C). Moreover, miR-876-3p ($r = 0.8634$, $p < 0.001$) and miR-876-5p ($r = 0.8179$, $p < 0.001$) expression level was positively associated with lncLingo2 expression (Figure 5D).

For investigating the function of mature miR-876 within the acquisition of morphine CPP, we delivered miR-876-3p (Figure 5E left), and miR-876-5p (Figure 5E right) mimics into NAcC, respectively. The results of two-way ANOVA exhibited a statistically significant main impact on CPP scores for morphine treatments ($F_{1,21} = 43.64$, $p < 0.001$) but not for upregulation of miR-876-3p within NAcC ($F_{1,21} = 0.3611$, $p = 0.5544$), and no interaction of morphine treatments × upregulation of miR-876-3p in NAcC (F1,21 = 0.5315, $p = 0.4740$). However, the results showed a significant main effect on CPP scores for morphine treatments ($F_{1,24} = 20.46$, $p < 0.001$) and upregulation of miR-876-5p in NAcC ($F_{1,24} = 6.639$, $p = 0.0166$). Moreover, interactions of morphine treatments × overexpression of miR-876-5p have been observed within NAcC ($F_{1,24} = 17.66$, $p < 0.001$). The resulting post hoc test demonstrated that viral-mediated overexpression of miR-876-5p ($p < 0.001$) within the NAcC significantly suppressed the acquisition of morphine-stimulated CPP while miR-876-3p overexpression ($p > 0.05$). The NAcS did not alter the CPP score in test 2. The aforementioned findings indicated that miR-876-5p, but not miR-876-3p, suppressed the acquisition of morphine CPP.

3.6 | MiR-876-5p regulates *Kcnn3* expression in NAcC of morphine CPP mice

The mRNA targets of miR-876-5p, which anticipated from miRDB, TargetScan and microT-CDS database, are shown in a Venn diagram in Figure 6A. We selected four miR-876-5p targeting mRNAs which were highly relevant to neuronal functions and regulation of neuronal plasticity in GO pathways analysis. According to the qRT-PCR results, the transcriptional abundance of *kcnn3* mRNA significantly increased in NAcC following morphine CPP training ($p < 0.001$, Figure 6B). Moreover, the level of miR-876-5p was inversely associated with *Kcnn3* mRNA expression within morphine trained mice (Figure 6C,D). Figure 6E illustrates that *Kcnn3* mRNA shared two 7-mer seed matches in its 3′ UTR with miR-876-5p, the target sequence of *Kcnn3* 3′ UTR and a conserved seed region-mutated sequence were subjected to luciferase assay in HEK293 cells. The results obtained from one-way ANOVA exhibited a statistically significant variation within groups on relative luciferase activity ($F_{3,8} = 63.28$, $p < 0.001$). The resulting post hoc tests revealed that mimics of miR-876-5p reduced the related luciferase activity ($p < 0.001$) (Figure 6F). Moreover, delivering of miR-876-5p mimics into NAcC significantly reduced the expression of *Kcnn3*.

Then, we detected the level of *Kcnn3* expression in NAcC of morphine-trained mice and evaluated the impact of miR-876-5p mimics on morphine CPP training-induced alteration of *Kcnn3* expression. Figure 6G illustrates that one-way ANOVA exhibited a statistically significant variation within groups on *Kcnn3* expression ($F_{3,8} = 11.47$, $p = 0.0029$). Post hoc investigations indicated that the expression of *Kcnn3* significantly elevated in NAcC of morphine-trained mice ($p = 0.0128$), and microinjection of miR-876-5p mimics into NAcC of morphine-trained mice inhibited the elevation of *Kcnn3* expression in NAcC after morphine CPP training ($p = 0.0307$) (Figure 6G).

3.7 | Overexpression of lncLingo2 inhibits neuronal excitability by regulating SK channel currents in NAcC of morphine CPP mice

Based on the observation that the elevated *Kcnn3* expression in NAcC after morphine CPP training was modulated by lncLingo2-derived miR-876-5p, we next determined if the SK channel currents in neurons were regulated by lncLingo2 in NAcC. Therefore, the whole-cell patch clamp method was employed for evaluating the SK channel current and neuronal excitability in NAcC of CPP training mice and investigated the impact of lncLingo2 upregulation on CPP training-stimulated alterations within electrophysiology characters (Figure 7A). The SK channel current emerges as a tail current which is a constituent of I_{AHP} that indicates the gradual deactivation of ion channels afterhyperpolarization (Figure 7B,C).[28] Two-way ANOVA analysis demonstrated that lncLingo2 overexpression exhibited a significant impact on the tail current mediated by SK channels (Figure 7D). It was observed that lncLingo2 overexpression reversed the elevated amplitude of tail current induced by morphine CPP training when the membrane potential outcome was depolarized from −50 to 0 mV (Groups: $F_{2,41} = 130$, $p < 0.001$; voltage: $F_{5,205} = 686.8$, $p < 0.001$). Moreover, one-way ANOVA analysis exhibited a statistically significant variation among groups on the amplitude of SK channel-mediated tail current at −20 mV ($F_{2,41} = 59.08$, $p < 0.001$). Post hoc tests revealed that the amplitude of SK channel-mediated tail current significantly increased after CPP training and was obviously diminished by lncLingo2 overexpression (Morphine+LV-Scramble vs. Saline: $p < 0.001$, LV-lncLingo2 vs. Morphine+LV-Scramble: $p < 0.001$) (Figure 7C,E).

FIGURE 5 MiR-876-5p derived from lncLingo2 regulates the acquisition of morphine CPP. (A) Prediction of secondary structure categories contained the sequence of pre-miR-876, which is labelled by the red identifiers. (B) miR-876 precursor and mature miR-876 expression level significantly elevated after overexpression of LncLingo2 by LV-LncLingo2 transfection in HEK293 cells ($n = 3$ per group). ***$p < 0.001$ vs. LV-scramble. (C) The expression of lncLingo2 in NAcC (right), but not in NAcS (left), decreased in a time-dependent manner ($n = 5$ per group). ***$p < 0.05$; ***$p < 0.001$ vs. saline group. (D) The expression of miR-876-3p (left) and miR-876-5p (right) in NAcC was positively correlated with lncLingo2 expression ($n = 16$). (E) Delivering miR-876-5p mimics (right) into NAcC inhibited the acquisition of morphine CPP while miR-876-3p mimics (left) did not yield any significant impact on CPP scores ($n = 6$–8 per group). ***$p < 0.001$ vs. miR negative group in morphine-trained mice.

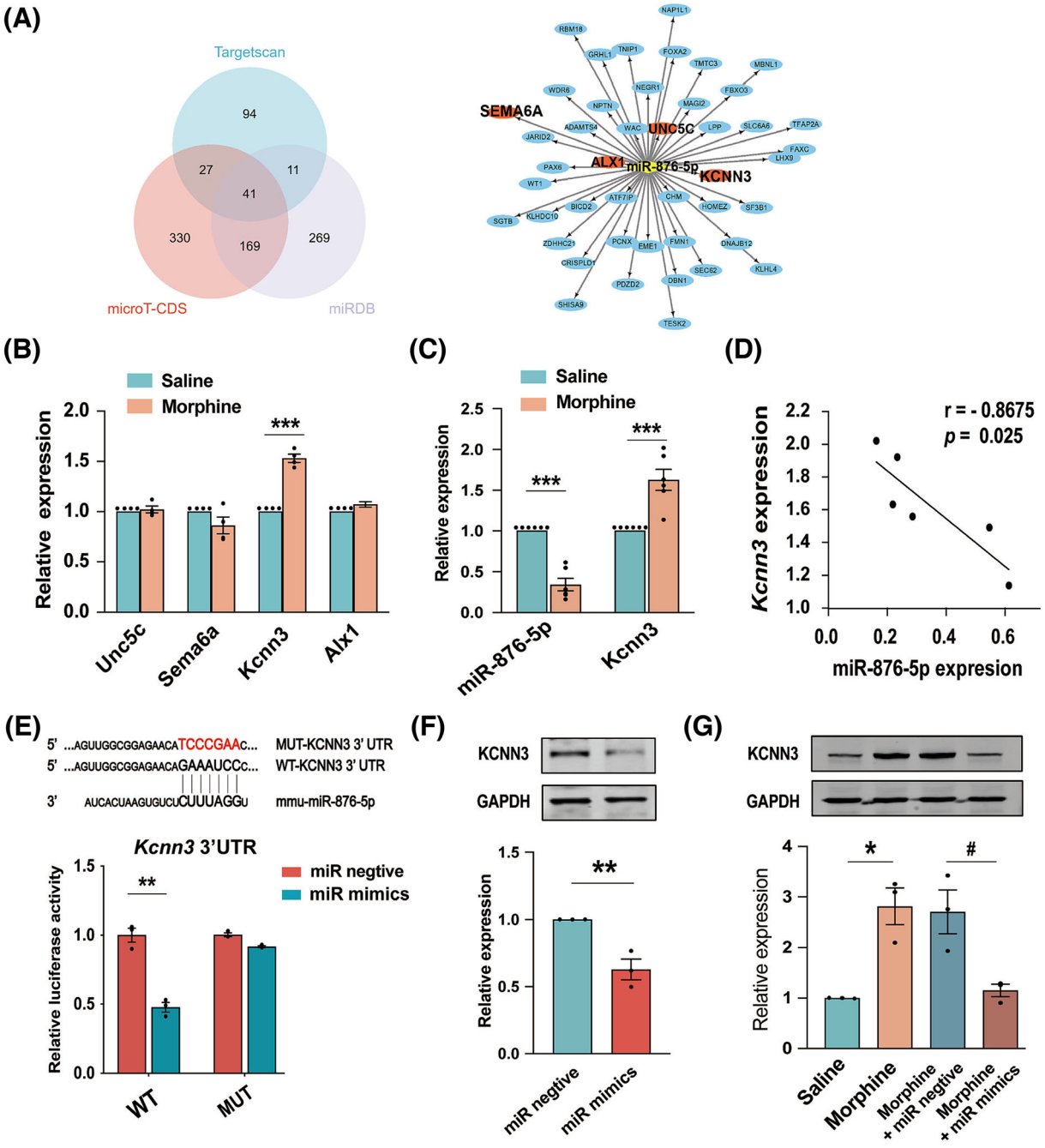

FIGURE 6 MiR-876-5p regulates *Kcnn3* expression in NAcC of morphine CPP mice. (A) Venn diagram showed the mRNA targets of miR-876-5p anticipated by miRDB, TargetScan and microT-CDS database (left). Four MiR-876-5p targeting mRNA highly relevant to neuronal functions and regulation of neuronal plasticity in GO enrichment analysis (right). (B) The transcript abundance of *kcnn3* mRNA significantly increased in NAcC after morphine CPP training ($n = 3$ per group). ***$p < 0.001$ vs. saline group. (C) The change of miR-876-5p and *kcnn3* mRNA expression in NAcC after morphine CPP training ($n = 3$ per group). ***$p < 0.001$ vs. saline group. (D) The level of miR-876-5p was inversely correlated with *Kcnn3* mRNA expression ($n = 6$). (E) The results of dual-luciferase reporter assay revealed that there was no significant alteration in relative luciferase activity in HEK293 cells upon mutation of the miR-876-5p binding sites located in the 3′ UTR of *kcnn3* gene. **$p < 0.01$ vs. miR negative. (F) Delivering miR-876-5p mimics into NAcC significantly reduced the expression of KCNN3 in naïve mice ($n = 3$ per group). **$p < 0.01$ vs. miR negative. (G) Microinjection of miR-876-5p mimics into NAcC of morphine-trained mice inhibited the elevation of *Kcnn3* expression in NAcC after morphine CPP training. ($n = 3$ per group). *$p < 0.05$ vs. saline group. $^{\#}p < 0.05$ vs. miR negative group in morphine-trained mice.

The neurons intrinsic excitability is closely related to the amplitude of afterhyperpolarization (AHP), involving the medium AHP (mAHP) and fast AHP (fAHP), which are regulated by SK channels and big-conductance calcium-activated potassium channels (BK channels), respectively.[29] Then we employed the whole-cell patch clamp assessment to measure the current injections induced AP and the AHP

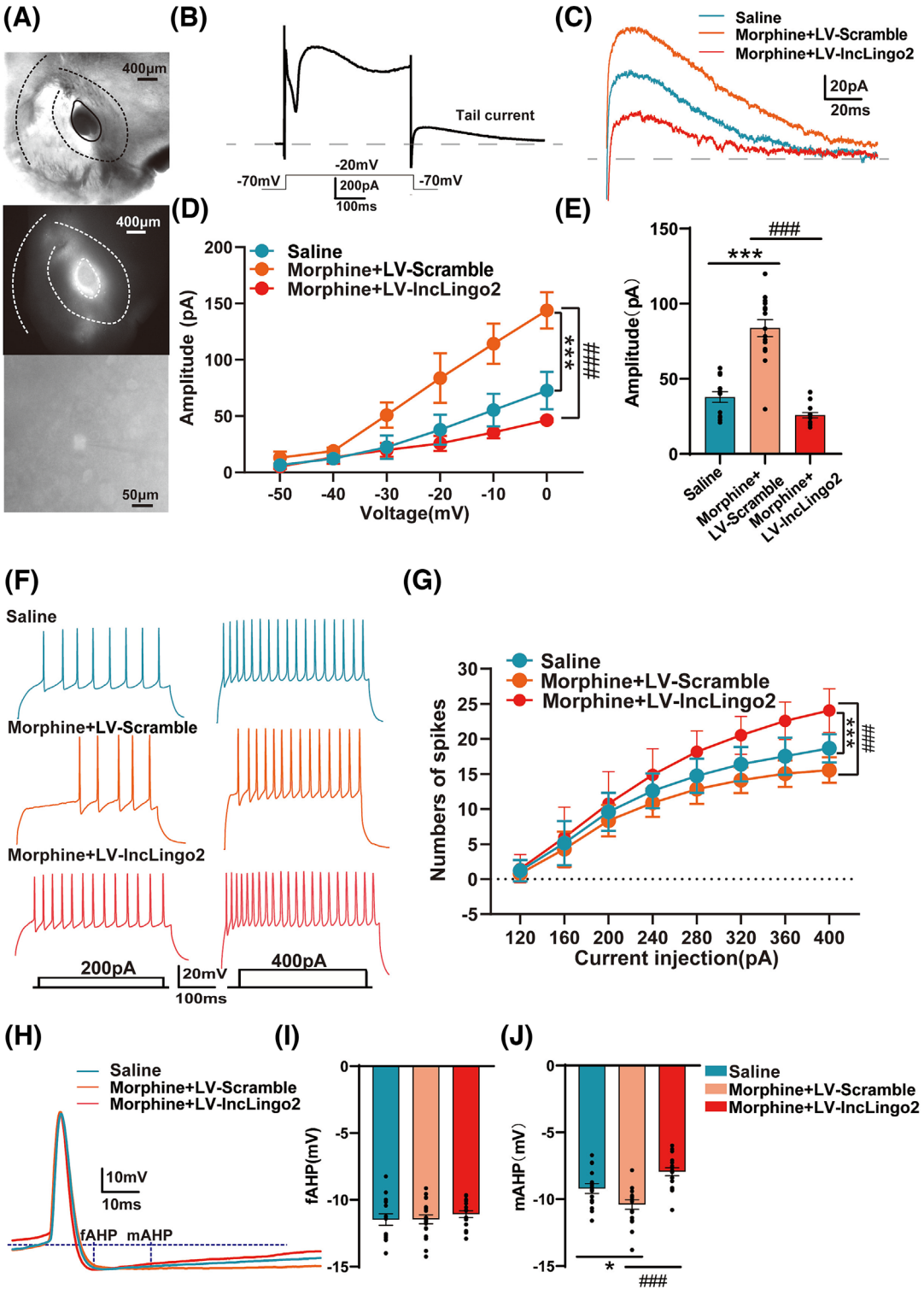

FIGURE 7 Legend on next page.

amplitude in NAcC (Figure 7F,H). The results of two-way ANOVA analysis showed that the decrease in AP firing evoked by injected current from 200 to 400 pA, which was caused by CPP training, was markedly reversed by lncLingo2 overexpression (Groups: $F_{2,47} = 17.5$, $p < 0.001$; current injection: $F_{7,329} = 1{,}062$, $p < 0.001$) (Figure 7G). Furthermore, the application of one-way ANOVA analysis demonstrated a statistically significant variation among the groups in terms of the amplitude of mAHP ($F_{2,47} = 13.58$, $p < 0.001$). Post hoc investigations demonstrated that a significantly elevated amplitude of mAHP was detected in NAcC from the CPP training group when compared to the saline group. Interestingly, the lncLingo2-overexpressing group exhibited a return to baseline levels (Morphine+LV-Scramble vs. Saline: $p < 0.01$, LV-lncLingo2 vs. Morphine+LV-Scramble: $p < 0.001$) (Figure 7I). However, no significant variation was observed within the fAHP of NAcC between the various groups (Figure 7H). These results indicate that lncLingo2 upregulation suppresses the low excitability of NAcC neurons by regulating SK3 channel currents in morphine CPP mice.

4 | DISCUSSION

lncRNAs exhibit several distinguishing features when compared to mRNAs. These features include a reduced number of exons, lesser conservation across evolutionary time and lower overall expression levels. However, lncRNAs have a higher degree of specificity in terms of their expression patterns within cells and tissues.[30] Among lncRNAs, about 40% are expressed specifically in the brain, underscoring the importance of studying their influence on neural function.[20,31] Throughout the current investigation, we initially screened a series of differentially expressed lncRNAs in NAc of morphine CPP training mice based on RNA-seq data and demonstrated lncLingo2 as a highly differential expressed lncRNA in NAcC, but not in NAcS, after morphine CPP and heroin IVSA training. Notably, the results also provide compelling evidence that lncLingo2 and its derived miR-876-5p in NAcC performed a crucial function in the formation of drug memory and the acquisition of opioid-associated behaviours.

The investigation of neural and molecular pathways affecting the formation of associative memories attached to opioids holds promise for advancing treatment approaches aimed at preventing and reversing drug addiction. Increasing evidence indicates that modulation of ncRNAs performs an essential function in neurodevelopment, neurodegenerative diseases and mental diseases.[32–35] Moreover, recent studies discovered substantial modifications in the expression profiles of ncRNA owing to drug exposure and clarified the functions of several specific ncRNAs in drug addiction,[36–38] and the dysregulation of lncRNAs has been observed and characterized within the NAc of mice that were subjected to treatment with methamphetamine and cocaine, as well as in the midbrain of individuals with a history of cocaine usage.[22,39] Previously, we examined the differential expression of lncRNAs, miRNAs and mRNAs within the NAc of morphine post-conditioning tested mice and predicted a comprehensive lncRNA-mediated ceRNA network underlying the reconsolidation of morphine-induced drug memory.[23] Herein, we profiled the changes of lncRNAs in NAc of morphine CPP-trained mice and found that lncLingo2 was region-specifically and time-specifically decreased in NAcC after morphine CPP conditioning and heroin IVSA training. Moreover, due to the expression changes of lncLingo2 and miR-876-5p occurred in the critical time window (6 h) of memory formation and morphine treatment without CPP training did not affect the NAcC lncLingo2 expression, we assumed that NAcC lncLingo2 might perform a specific function in the formation of opioids-related contextual memory.

The mesolimbic DA pathway which consists of the ventral tegmental area (VTA) and its corresponding DAergic neuronal projections to the NAc,[40,41] and the glutamatergic projections from the VTA to the NAc and from the IL/PrL to the NAc has consistently been recognized as an important neural circuit underlying the drug dependency.[42] Furthermore, the NAcC and NAcS, which are two subregions of the NAc, are recognized to possess separate functions in relation to drug-related behaviours. The NAcC is essential for the retention of rewarding information derived from conditioned drug stimulus, whereas the NAcS is implicated in the motor-activating consequences of addictive drugs.[43] Throughout the current investigation, we explored the function of NAc lncLingo2 in the acquisition of opioids-associated behaviours using morphine CPP and heroin IVSA, two complementary paradigms to evaluate drug-associated memories. The results revealed that lncLingo2 expression significantly decreased in

FIGURE 7 Overexpression of lncLingo2 inhibits neuronal excitability by regulating SK3 channel currents in NAcC of morphine CPP mice. (A) Representative images of AAV virus injection sites in NAcC and the neuron labelled utilizing mCherry in NAcC patched with a micropipette. The dotted lines represent the boundaries of NAcC and NAcS. (B) A representative trace of the depolarized current and the SK channels mediated tail current in voltage-clamp mode. (C) Representative traces of mediated SK channels mediated tail current in NAcC neuron. (D) The amplitude of SK channels mediated tail current induced by depolarization from −50 to 0 mV increased after CPP training and could be reflected by lncLingo2 upregulation. ($n = 14$–15 cells from six mice per group, $^{***}p < 0.001$ vs. saline group; $^{###}p < 0.001$ vs. LV-scramble group). (E) The amplitude of SK channels mediated tail current at −20 mV holding potential increased after CPP training but has been significantly diminished following lncLingo2 overexpression ($^{***}p < 0.001$ vs. saline group; $^{###}p < 0.001$ vs. LV-scramble group). (F) Representative traces of evoked potential induced by 200 and 400 pA current injections in NAcC neurons. (G) The elevation of injected current-dependent AP firing in NAcC neurons induced by CPP training was significantly reflected by lncLingo2 upregulation ($n = 14$–15 cells from six mice, $^{***}p < 0.001$ vs. saline group; $^{###}p < 0.001$ vs. LV-scramble group). (H) Representative traces of evoked potential. (I) There is no significant variation in fAHP among groups ($n = 14$–15 cells from six mice per group). (J) The amplitude of mAHP in NAcC neuron increased after CPP training but was reversed by lncLingo2 overexpressed ($n = 14$–15 cells from six mice per group, $^{**}p < 0.01$ vs. saline group; $^{###}p < 0.001$ vs. LV-scramble group). Data are presented as the mean ± SEM.

NAcC but not in NAcS of morphine CPP-trained mice. Overexpression of lncLingo2 in NAcC by LV-lncLingo2 substantially suppressed the attainment of morphine-induced CPP and heroin-induced IVSA. Moreover, there was no variation found among LV-lncLingo2 and LV-scramble transfected mice in the locomotion test, which indicated that overexpression of lncLingo2 did not affects spontaneous activity. As known, the SA paradigms are also widely used to assess the rewarding motivational effects and emotional memory induced by various stimuli, including drugs and food. To investigate the specificity role of lncLingo2 disturbance in opioids-induced drug-associated behaviours, the expression of lncLingo2 in NAcC was determined in high glucose pellets SA-trained mice. Interestingly, the expression of lncLingo2 did not alter after the above training procedure, which indicated that lncLingo2 might not be related to natural rewarding stimulus-induced contextual memory.

A substantial body of evidence demonstrates that lncRNAs regulate gene expression in multiple patterns.[44,45] Of note, it can potentially acquire activity by serving as precursors of small RNAs that possess regulatory capabilities, including miRNAs.[46,47] By performing the RACE assay, we acquired the full-length information of lncLingo2. According to the results of subcellular fractionation detection of lncLingo2 and secondary structure prediction by bioinformatic analysis, it is supposed that lncLingo2 might exert its function by deriving miR-876-5p. In order to provide further clarification to this hypothesis, the level of miR-876-5p expression after lncLingo2 overexpression was detected in HEK293 cells due to they do not express lncLingo2 under normal conditions. It was observed that the expression of precursor (pre-miR-876) and mature miR-876-3p and miR-876-5p in HEK293 cells was also increased after lncLingo2 overexpression by LV-lncLingo2 transfection. In morphine-trained mice, pre-miR-876, miR-876-3p and miR-876-5p expression levels within NAcC decreased in a time-dependent manner after CPP training but had no change in NAcS, and the level of miR-876-3p and miR-876-5p expression were positively correlated with lncLingo2. Subsequently, we explored the function of miR-876-3p and miR-876-5p in the acquisition of opioid-associated behaviours. Interestingly, only miR-876-5p mimics microinjection into NAcC suppressed the acquisition of morphine CPP. Overall, this piece of result is the first one to demonstrate the function of lncLingo2, and it derived miR-876-5p in the acquisition of opioid-associated behaviours.

Like other transcriptional regulators, miRNAs exhibit the characteristic behaviour of binding to the 3′ UTR of target mRNAs, hence inhibiting their translation and facilitating their destruction. The prediction of target genes for miR-876-5p was conducted using miRDB, TargetScan and microT-CDS databases. To explore the molecular funtions of 41 target genes, GO funtional annotation and pathway enrichment was performed using David and Funrich, where Kcnn3, Sema6A, Unc5c and Alx1 genes were closely related to neuronal differentiation, axonal growth and addiction. However, only the expression of *Kcnn3* was increased in the NAcC after morphine CPP training as determined by the qRT-PCR. Based on the anticipated binding sites of miR-876-5p in *the Kcnn3* gene, dual-luciferase reporter assays demonstrated the interaction of miR-876-5p and *Kcnn3* mRNA. In addition, delivering miR-876-5p mimics into NAcC significantly decreased the expression of *Kcnn3* in naïve mice and inhibited the elevation of *Kcnn3* expression in NAcC after morphine CPP training. The *Kcnn3* gene is responsible for encoding the small-conductance calcium-activated potassium channel 3 (SK3 channel). Three cloned SK channel subunits (SK1, SK2 and SK3) have distinct distributions in the central nervous system and different physiological and pharmacological features. These features play a crucial role in regulating neuronal firing frequency and spike frequency adaptation.[48,49] It has been reported that the SK3 channel is involved in the generation of slow posterior hyper chemical potential, which affects the calcium-mediated series of intracellular effects by regulating excitatory and non-excitatory cell membrane action potentials.[50,51] SK3 channel also can affect the activity of dopamine (DA) and serotonin (HT)-ergic neurons, performing critical functions in neurotransmission, synaptic plasticity regulation, learning and memory.[52–55] Moreover, it has been reported that the SK3 channel is involved in the generation of slow posterior hyper chemical potential, which affects the calcium-mediated series of intracellular effects by regulating excitatory and non-excitatory cell membrane action potentials.[50,51] Based on these findings, we further performed whole-cell patch clamp experiments to observe the SK channel currents and intrinsic excitability of neurons after morphine CPP training. We found increasing SK channel currents with increasing SK3 expression after morphine CPP training. The SK channel currents perform an essential function in regulating the firing of action potentials (APs) and are considered potent modulators in this process. They are an integral part of the I_{mAHP}, which is responsible for modulating neuronal excitability.[56,57] Herein, the excitability of NAcC neurons significantly decreased, and the amplitude of I_{mAHP} elevated after morphine CPP training, which both were markedly reversed by lncLingo2 overexpression-induced downregulation of *Kcnn3* expression.

However, this study still has limitations due to study design. Although we concluded an important role of lncLingo2 and it derived miR-876-5p in the acquisition of opioids-associated behaviours, the network function of lncLingo2 – miR-876-5p and its target *Kcnn3* gene in the formation of opioids-associated contextual memory needs to be further clarified. Moreover, another limitation of this study is that the gene manipulation on lncLingo2 in NAc for functional verification should be specific to cell types. The cholinergic interneurons (CINs) and parvalbumin (PV) interneurons are also distributed in NAc, which play roles in the modulation of MSNs excitability and synaptic transmission.[58,59] We also highlighted the complexity of lncRNAs and miRNAs throughout the modulation of gene expression process. The other target genes of lncLingo2 and the upstream signalling that lead to lncLingo2 downregulation should be investigated within the subsequent investigations.

Collectively, the findings of our research suggest that lncLingo2 and its derived miR-876-5p perform an essential function in the acquisition of opioids-associated behaviours, and the gain of lncLingo2 or miR-876-5p function suppresses the acquisition of opioids-associated behaviours and the corresponding elevation of *Kcnn3* gene expression related to the excitability of NAcC

neurons. This discovery has the potential to enhance our comprehension of the molecular pathways that underlie behaviours related to opioids.

AUTHOR CONTRIBUTIONS

DW, CLM and YXL designed this work. HYY, MLZ and DW drafted the manuscript. BC revised the manuscript. HYY, XNZ, YL and HLY conducted animal investigations. MLZ conducted electrophysiology and western blot analysis. The data were evaluated and interpreted by BX and SGS. The manuscript was reviewed, amended and granted approval from all authors.

ACKNOWLEDGEMENTS

The current investigation has received financial support from the National Natural Science Foundation of China [No. 81971785] and the Natural Science Foundation of Hebei Province [No. H2022206026].

CONFLICT OF INTEREST STATEMENT

The authors do not have any conflicts of interest to disclose.

DATA AVAILABILITY STATEMENT

The datasets analysed in this manuscript are not publicly available. Requests to access the datasets should be directed to wendi01125@126.com.

ORCID

Minglong Zhang https://orcid.org/0009-0007-6627-0774
Bin Cong https://orcid.org/0000-0003-3325-371X

REFERENCES

1. Robbins TW, Ersche KD, Everitt BJ. Drug addiction and the memory systems of the brain. *Ann N Y Acad Sci*. 2008;1141(1):1-21. doi:10.1196/annals.1441.020
2. Berke JD. Learning and memory mechanisms involved in compulsive drug use and relapse. *Methods Mol Med*. 2003;79:75-101. doi:10.1385/1-59259-358-5:75
3. Xue YX, Luo YX, Wu P, et al. A memory retrieval-extinction procedure to prevent drug craving and relapse. *Science*. 2012;336(6078):241-245. doi:10.1126/science.1215070
4. Schroeder JP, Packard MG. Facilitation of memory for extinction of drug-induced conditioned reward: role of amygdala and acetylcholine. *Learn Mem*. 2004;11(5):641-647. doi:10.1101/lm.78504
5. Liu JF, Tian J, Li JX. Modulating reconsolidation and extinction to regulate drug reward memory. *Eur J Neurosci*. 2019;50(3):2503-2512. doi:10.1111/ejn.14072
6. Taujanskaite U, Cahill EN, Milton AL. Targeting drug memory reconsolidation: a neural analysis. *Curr Opin Pharmacol*. 2021;56:7-12. doi:10.1016/j.coph.2020.08.007
7. Haroutunian V, Riccio DC. Drug-induced "arousal" and the effectiveness of CS exposure in the reinstatement of memory. *Behav Neural Biol*. 1979;26(1):115-120. doi:10.1016/s0163-1047(79)92959-5
8. Liang J, Li JL, Han Y, et al. Calpain-GRIP signaling in nucleus accumbens core mediates the reconsolidation of drug reward memory. *J Neurosci*. 2017;37(37):8938-8951. doi:10.1523/JNEUROSCI.0703-17.2017
9. Luo YX, Xue YX, Shen HW, Lu L. Role of amygdala in drug memory. *Neurobiol Learn Mem*. 2013;105:159-173. doi:10.1016/j.nlm.2013.06.017
10. Robbins TW, Everitt BJ. Limbic-striatal memory systems and drug addiction. *Neurobiol Learn Mem*. 2002;78(3):625-636. doi:10.1006/nlme.2002.4103
11. Kobrin KL, Moody O, Arena DT, Moore CF, Heinrichs SC, Kaplan GB. Acquisition of morphine conditioned place preference increases the dendritic complexity of nucleus accumbens core neurons. *Addict Biol*. 2016;21(6):1086-1096. doi:10.1111/adb.12273
12. Lv X-F, Sun L-L, Cui C-L, Han J-S. NAc shell arc/Arg3.1 protein mediates reconsolidation of morphine CPP by increased GluR1 cell surface expression: activation of ERK-coupled CREB is required. *Int J Neuropsychopharmacol*. 2015;18(9):pyv030. doi:10.1093/ijnp/pyv030
13. Shen F, Wang N, Qi C, Li YJ, Cui CL. The NO/sGC/PKG signaling pathway in the NAc shell is necessary for the acquisition of morphine-induced place preference. *Behav Neurosci*. 2014;128(4):446-459. doi:10.1037/a0036964
14. Zhao J, Ying L, Liu Y, et al. Different roles of Rac1 in the acquisition and extinction of methamphetamine-associated contextual memory in the nucleus accumbens. *Theranostics*. 2019;9(23):7051-7071. doi:10.7150/thno.34655
15. Campbell RR, Kramar EA, Pham L, et al. HDAC3 activity within the nucleus accumbens regulates cocaine-induced plasticity and behavior in a cell-type-specific manner. *J Neurosci*. 2021;41(13):2814-2827. doi:10.1523/JNEUROSCI.2829-20.2021
16. Wang YQ, Huang YH, Balakrishnan S, et al. AMPA and NMDA receptor trafficking at cocaine-generated synapses. *J Neurosci*. 2021;41(9):1996-2011. doi:10.1523/JNEUROSCI.1918-20.2021
17. Nestler EJ. Epigenetic mechanisms of drug addiction. *Neuropharmacology*. 2014;76(Pt B(0 0)):259-268. doi:10.1016/j.neuropharm.2013.04.004
18. Sartor GC, St Laurent G 3rd, Wahlestedt C. The emerging role of non-coding RNAs in drug addiction. *Front Genet*. 2012;3:106. doi:10.3389/fgene.2012.00106
19. Bu Q, Long H, Shao X, et al. Cocaine induces differential circular RNA expression in striatum. *Transl Psychiatry*. 2019;9(1):199. doi:10.1038/s41398-019-0527-1
20. Clark BS, Blackshaw S. Long non-coding RNA-dependent transcriptional regulation in neuronal development and disease. *Front Genet*. 2014;5:164. doi:10.3389/fgene.2014.00164
21. Bu Q, Hu Z, Chen F, et al. Transcriptome analysis of long non-coding RNAs of the nucleus accumbens in cocaine-conditioned mice. *J Neurochem*. 2012;123(5):790-799. doi:10.1111/jnc.12006
22. Zhu L, Zhu J, Liu Y, et al. Methamphetamine induces alterations in the long non-coding RNAs expression profile in the nucleus accumbens of the mouse. *BMC Neurosci*. 2015;16(1):18. doi:10.1186/s12868-015-0157-3
23. Li X, Xie B, Lu Y, et al. Transcriptomic analysis of long non-coding RNA-MicroRNA-mRNA interactions in the nucleus accumbens related to morphine addiction in mice. *Front Psych*. 2022;13:915398. doi:10.3389/fpsyt.2022.915398
24. Gao S, Li E, Gao H. Long non-coding RNA MEG3 attends to morphine-mediated autophagy of HT22 cells through modulating ERK pathway. *Pharm Biol*. 2019;57(1):536-542. doi:10.1080/13880209.2019.1651343
25. Browne CJ, Godino A, Salery M, Nestler EJ. Epigenetic mechanisms of opioid addiction. *Biol Psychiatry*. 2020;87(1):22-33. doi:10.1016/j.biopsych.2019.06.027
26. Guo C, Wen D, Zhang Y, et al. Amyloid-beta oligomers in the nucleus accumbens decrease motivation via insertion of calcium-permeable AMPA receptors. *Mol Psychiatry*. 2022;27(4):2146-2157. doi:10.1038/s41380-022-01459-0

27. Zhang M, Luo Y, Wang J, et al. Roles of nucleus accumbens shell small-conductance calcium-activated potassium channels in the conditioned fear freezing. *J Psychiatr Res*. 2023;163:180-194. doi:10.1016/j.jpsychires.2023.05.057
28. Cannady R, McGonigal JT, Newsom RJ, Woodward JJ, Mulholland PJ, Gass JT. Prefrontal cortex K Ca2 channels regulate mGlu5-dependent plasticity and extinction of alcohol-seeking behavior. *J Neurosci*. 2017;37(16):4359-4369. doi:10.1523/jneurosci.2873-16.2017
29. Shan L, Galaj E, Ma YY. Nucleus accumbens shell small conductance potassium channels underlie adolescent ethanol exposure-induced anxiety. *Neuropsychopharmacology*. 2019;44(11):1886-1895. doi:10.1038/s41386-019-0415-7
30. Cabili MN, Trapnell C, Goff L, et al. Integrative annotation of human large intergenic noncoding RNAs reveals global properties and specific subclasses. *Genes Dev*. 2011;25(18):1915-1927. doi:10.1101/gad.17446611
31. Cao X, Yeo G, Muotri AR, Kuwabara T, Gage FH. Noncoding RNAs in the mammalian central nervous system. *Annu Rev Neurosci*. 2006;29(1):77-103. doi:10.1146/annurev.neuro.29.051605.112839
32. Faghihi MA, Modarresi F, Khalil AM, et al. Expression of a noncoding RNA is elevated in Alzheimer's disease and drives rapid feed-forward regulation of beta-secretase. *Nat Med*. 2008;14(7):723-730. doi:10.1038/nm1784
33. Mehler MF, Mattick JS. Noncoding RNAs and RNA editing in brain development, functional diversification, and neurological disease. *Physiol Rev*. 2007;87(3):799-823. doi:10.1152/physrev.00036.2006
34. Hao WZ, Chen Q, Wang L, et al. Emerging roles of long non-coding RNA in depression. *Prog Neuropsychopharmacol Biol Psychiatry*. 2022;115:110515. doi:10.1016/j.pnpbp.2022.110515
35. Zakutansky PM, Feng Y. The long non-coding RNA GOMAFU in schizophrenia: function, disease risk, and beyond. *Cell*. 2022;11(12):1949. doi:10.3390/cells11121949
36. Zhu L, Wu F, Yan Z, et al. A novel microRNA, novel-m009C, regulates methamphetamine rewarding effects. *Mol Psychiatry*. 2022;27(9):3885-3897. doi:10.1038/s41380-022-01651-2
37. Xie B, Zhang J, Ma C, et al. Roles of miR-592-3p and its target gene, TMEFF1, in the nucleus accumbens during incubation of morphine craving. *Int J Neuropsychopharmacol*. 2022;25(5):412-424. doi:10.1093/ijnp/pyac004
38. Yu H, Xie B, Zhang J, et al. The role of circTmeff-1 in incubation of context-induced morphine craving. *Pharmacol Res*. 2021;170:105722. doi:10.1016/j.phrs.2021.105722
39. Bannon MJ, Savonen CL, Jia H, et al. Identification of long noncoding RNAs dysregulated in the midbrain of human cocaine abusers. *J Neurochem*. 2015;135(1):50-59. doi:10.1111/jnc.13255
40. Self DW. Regulation of drug-taking and -seeking behaviors by neuroadaptations in the mesolimbic dopamine system. *Neuropharmacology*. 2004;47(Suppl 1):242-255. doi:10.1016/j.neuropharm.2004.07.005
41. Mameli M, Halbout B, Creton C, et al. Cocaine-evoked synaptic plasticity: persistence in the VTA triggers adaptations in the NAc. *Nat Neurosci*. 2009;12(8):1036-1041. doi:10.1038/nn.2367
42. Ma YY, Lee BR, Wang X, et al. Bidirectional modulation of incubation of cocaine craving by silent synapse-based remodeling of prefrontal cortex to accumbens projections. *Neuron*. 2014;83(6):1453-1467. doi:10.1016/j.neuron.2014.08.023
43. Ito R, Robbins TW, Everitt BJ. Differential control over cocaine-seeking behavior by nucleus accumbens core and shell. *Nat Neurosci*. 2004;7(4):389-397. doi:10.1038/nn1217
44. Khalil AM, Guttman M, Huarte M, et al. Many human large intergenic noncoding RNAs associate with chromatin-modifying complexes and affect gene expression. *Proc Natl Acad Sci U S A*. 2009;106(28):11667-11672. doi:10.1073/pnas.0904715106
45. Kurokawa R. Promoter-associated long noncoding RNAs repress transcription through a RNA binding protein TLS. *Adv Exp Med Biol*. 2011;722:196-208. doi:10.1007/978-1-4614-0332-6_12
46. Lee JT. Epigenetic regulation by long noncoding RNAs. *Science*. 2012;338(6113):1435-1439. doi:10.1126/science.1231776
47. Mercer TR, Mattick JS. Structure and function of long noncoding RNAs in epigenetic regulation. *Nat Struct Mol Biol*. 2013;20(3):300-307. doi:10.1038/nsmb.2480
48. Sailer CA, Kaufmann WA, Marksteiner J, Knaus HG. Comparative immunohistochemical distribution of three small-conductance Ca2+-activated potassium channel subunits, SK1, SK2, and SK3 in mouse brain. *Mol Cell Neurosci*. 2004;26(3):458-469. doi:10.1016/j.mcn.2004.03.002
49. Stocker M, Pedarzani P. Differential distribution of three Ca(2+)-activated K(+) channel subunits, SK1, SK2, and SK3, in the adult rat central nervous system. *Mol Cell Neurosci*. 2000;15(5):476-493. doi:10.1006/mcne.2000.0842
50. Liegeois JF, Mercier F, Graulich A, Graulich-Lorge F, Scuvee-Moreau J, Seutin V. Modulation of small conductance calcium-activated potassium (SK) channels: a new challenge in medicinal chemistry. *Curr Med Chem*. 2003;10(8):625-647. doi:10.2174/0929867033457908
51. Obermair GJ, Kaufmann WA, Knaus HG, Flucher BE. The small conductance Ca2+-activated K+ channel SK3 is localized in nerve terminals of excitatory synapses of cultured mouse hippocampal neurons. *Eur J Neurosci*. 2003;17(4):721-731. doi:10.1046/j.1460-9568.2003.02488.x
52. Blank T, Nijholt I, Kye MJ, Radulovic J, Spiess J. Small-conductance, Ca2+-activated K+ channel SK3 generates age-related memory and LTP deficits. *Nat Neurosci*. 2003;6(9):911-912. doi:10.1038/nn1101
53. Jacobsen JP, Weikop P, Hansen HH, et al. SK3 K+ channel-deficient mice have enhanced dopamine and serotonin release and altered emotional behaviors. *Genes Brain Behav*. 2008;7(8):836-848. doi:10.1111/j.1601-183X.2008.00416.x
54. Benitez BA, Belalcazar HM, Anastasia A, et al. Functional reduction of SK3-mediated currents precedes AMPA-receptor-mediated excitotoxicity in dopaminergic neurons. *Neuropharmacology*. 2011;60(7–8):1176-1186. doi:10.1016/j.neuropharm.2010.10.024
55. Qu L, Wang Y, Li Y, et al. Decreased neuronal excitability in medial prefrontal cortex during morphine withdrawal is associated with enhanced SK channel activity and upregulation of small GTPase Rac1. *Theranostics*. 2020;10(16):7369-7383. doi:10.7150/thno.44893
56. Kshatri AS, Gonzalez-Hernandez A, Giraldez T. Physiological roles and therapeutic potential of Ca(2+) activated potassium channels in the nervous system. *Front Mol Neurosci*. 2018;11:258. doi:10.3389/fnmol.2018.00258
57. Bock T, Honnuraiah S, Stuart GJ. Paradoxical excitatory impact of SK channels on dendritic excitability. *J Neurosci*. 2019;39(40):7826-7839. doi:10.1523/JNEUROSCI.0105-19.2019
58. Manz KM, Brady LJ, Calipari ES, Grueter BA. Accumbal histamine signaling engages discrete interneuron microcircuits. *Biol Psychiatry*. 2021;93(11):1041-1052. doi:10.1016/j.biopsych.2021.10.004
59. Xiao Q, Zhou X, Wei P, et al. A new GABAergic somatostatin projection from the BNST onto accumbal parvalbumin neurons controls anxiety. *Mol Psychiatry*. 2021;26(9):4719-4741. doi:10.1038/s41380-020-0816-3

How to cite this article: Yang H, Zhang X, Zhang M, et al. Roles of lncLingo2 and its derived miR-876-5p in the acquisition of opioid reinforcement. *Addiction Biology*. 2024;29(2):e13375. doi:10.1111/adb.13375.